

Supporting Information

Quantitative Reflection Imaging for Morphology and Dynamics of Live *Aplysia californica* Pedal Ganglion Neurons Cultured on Nanostructured Plasmonic Crystals

Somi Kang[†], *Adina Badea*[†], *Stanislav S. Rubakhin*^{‡,||}, *Jonathan V. Sweedler*^{‡,||}, *John A. Rogers*[†],
‡, and *Ralph G. Nuzzo*^{*,†,‡}

[†] Department of Materials Science and Engineering, University of Illinois at Urbana-Champaign, Urbana, Illinois 61801, United States of America

[‡] Department of Chemistry, University of Illinois at Urbana-Champaign, Urbana, Illinois 61801, United States of America

^{||} Beckman Institute for Advanced Science and Technology, University of Illinois at Urbana-Champaign, Urbana, Illinois 61801, United States of America

Supplementary Methods

Reagents. Reagents were used as received without further purification. Polydimethylsiloxane (soft PDMS; Sylgard 184, Dow Corning, Auburn, MI) was made in a 10:1 ratio of PDMS base with curing agent. Hard PDMS components: poly(25-30% methylhydrosiloxane)-(dimethylsiloxane) (HMS-301), poly(7-8% vinylmethylsiloxane)-(dimethylsiloxane), (VDT-731), Platinum divinyltetramethyldisiloxane (SIP6831.1) and (1,3,5,7-tetravinyl-1,3,5,7-tetramethylcyclotetrasiloxane) (7900) were purchased from Gelest (Morrisville, PA). Manganese chloride tetrahydrate, poly(sodium 4-styrenesulfonate) (PSS, MW = 70,000 g/mol), poly(allylamine hydrochloride) (PAH, MW = 70,000 g/mol), 16-mercaptohexadecanoic acid (MHDA), and trypsin (T1426) were purchased from Sigma-Aldrich (St. Louis, MO). Norland Optical Adhesive (NOA) was obtained from Norland Products Inc. (Cranbury, NJ). Ultrapure water (18 M Ω) was generated using a Millipore Milli-Q Academic A-10 system and used to prepare the polyelectrolyte solutions and artificial sea water (ASW).

Plasmonic Crystal Fabrication via Soft Nanoimprint Lithography. Full 3D plasmonic crystals were fabricated using soft nanoimprint lithography technique as previously reported.¹⁻⁶ First, a double-layer PDMS stamp (composite hard-PDMS/ soft-PDMS) was cast from a patterned photoresist master consisting of nanohole array relief structures and subsequently used to fabricate the plasmonic crystal. Several droplets of the NOA prepolymer was cast onto a glass slide by pressing the PDMS stamp into the liquid pre-polymer and then cured by exposing to ultraviolet light for ~20 min. After carefully peeling off the PDMS stamp, the NOA nanostructures were usually placed in a 70 °C oven overnight to complete curing with heat treatment. The replicated nanostructures were a uniform square array of nanoholes with a hole

spacing (center to center) of ~740 nm, a hole diameter of ~540 nm, and a relief depth of ~285 nm. After a sputtering procedure to deposit ~5 nm of titanium dioxide adhesion layer on top of the NOA nanohole array, ~45 nm of gold were deposited by sputter deposition in 5 mTorr argon (AJA International). To improve cell outgrowth on the plasmonic crystal and prevent water penetration at the interface between metal film and NOA nanostructures, a thin layer of aluminum oxide (Al_2O_3) of ~6 nm was deposited via ALD at 80°C at a deposition rate of 0.96 Å/s (atomic layer deposition, Cambridge Nanotech, Waltham, MA).

Transmission-mode Measurements of Plasmonic Crystals. Transmission spectra of plasmonic crystals were measured using a Cary 5G UV-Vis-NIR (Agilent, Santa Clara, CA) spectrophotometer at normal incidence. Transmission spectra over a wavelength range of 355-1200 nm were collected for use in further computational modeling.

Growth of Polyelectrolyte Layer-by-Layer Assemblies for Reflection Imaging Contrast Calibration. Polyelectrolyte assemblies were created on the surface of the plasmonic crystal or gold-coated pieces of a silicon wafer by a LBL method. To facilitate the LBL deposition, carboxylic acid-terminated self-assembled monolayers were formed on the gold film surface by immersing the substrates in an ethanol solution of MHDA (2 mM) for at least 18 h, after which the substrates were rinsed thoroughly with ethanol and dried under nitrogen flow. Layers of PAH and PSS were then alternately deposited onto the surface of the gold coated substrate. The substrate was immersed in a PAH solution (3 mg PAH/mL in water, pH = 8.0) for 5 min, rinsed thoroughly with water and dried with nitrogen gas. This PAH-layer terminated substrate was then immersed in a PSS solution (3 mg PSS/mL in 1M MnCl_2 , pH = 2.0) for 90 s, rinsed with water and dried under nitrogen flow.

Thickness and Refractive Index Measurements of Polyelectrolyte Layer-by-Layer (LBL) Assemblies in Artificial Sea Water (ASW) with Atomic Force Microscopy (AFM) and Ellipsometry. The thicknesses of polyelectrolyte LBL assemblies on gold-coated silicon in ASW were measured using an MFP-3D atomic force microscope (Asylum Research, Santa Barbara, CA) and the refractive indices of the polyelectrolyte films under the same conditions were determined using a VASE spectroscopic ellipsometer (J.A. Woollam Co., Lincoln, NE) with a home-built liquid cell (shown in Figure S1). To simplify the analysis, gold-coated silicon wafer pieces were used for the AFM and ellipsometry measurements, each examined after surface modification with a MHDA monolayer. AFM was used to directly measure the thickness of the polyelectrolyte layer in ASW. Areas of the gold-coated silicon were masked using permanent marker to delineate the pattern of the polyelectrolyte LBL assemblies. After removing the mask with acetone, the polyelectrolyte thickness was determined by measuring the edge step at the boundary of the polyelectrolyte covered and non-covered regions. These tapping mode AFM measurements were made in ASW using a soft cantilever (0.08 N/m spring constant, Asylum Research). Analysis of the AFM data was performed using IgorPro. The thickness data from the AFM measurement was used in calculations made to determine the refractive indices of the polyelectrolyte films based on ellipsometry data. At every second round of polyelectrolyte deposition, ellipsometry data were collected over the wavelength range of 300-900 nm at an incident angle of 60°. These were evaluated using a Cauchy model.

Reflection-mode Imaging Measurements. Reflection mode images of both the polyelectrolyte films and live cells in culture on the plasmonic crystal surface were obtained using a Zeiss AxioScope A1 microscope with halogen light source and a 20X, 0.40 NA objective. Bandpass filters were inserted in the microscope immediately in front of the microscope camera (AxioCam

MRc) and images captured using an AxioVision 1388 × 1040 pixels array camera (each pixel 6.5 × 6.5 μm). The imaging mode measurements were made in regions where essentially linear calibrations could be applied on the optical responses (although, the latter constraint is not mandated and other choices might be made to afford more sensitive responses to specific changes in the refractive index environment proximal to the plasmonic crystal). To do so, the bandpass filters used were 500-550nm (XF1074), 570-1000nm (BA414IF), 520-1000nm (BA414F), 570-600nm (580DF30), 600-700nm (XF3081), 415-485nm (10BF70_450), 515-585nm (10BF70_550), and 615-685nm (10BF70_650). The acquisition time was varied to control the overall exposure, with the halogen lamp intensity fixed at a low level to preclude thermal damage to the live cells.

Grayscale reflection images were processed and analyzed using Matlab and ImageJ. Vignetting in the images of the polyelectrolyte layer and the live cell cultures was corrected using a pixel-by-pixel division of the experimental image by a reference mirror image of the original plasmonic crystal taken with the corresponding bandpass filter. With the assumption that the contrast values of each pixel have a standard normal distribution, pixel values falling outside of the 80% confidential intervals were excluded from the reflection imaging contrast calibration.

Reflection Contrast Calibration. A portion of the MHDA-coated nanohole array was covered with a cured NOA film to create a region at which the surface refractive index remained unchanged during the polyelectrolyte film deposition. The reflection images of this plasmonic crystal were taken at every second round of the polyelectrolyte deposition to calibrate the normalized reflection contrast changes as a function of thickness of polyelectrolyte assemblies.

The normalized reflection contrasts for the coated regions were calculated using a method reported previously¹ using the relationships given in Equations (1) and (2):

$$\text{Scaled PEL average} = [\text{Image PEL average}] \times \frac{[\text{Reference NOA average}]}{[\text{Image NOA average}]} \quad (1)$$

$$\text{Normalized reflection contrast} = \frac{[\text{scaled PEL average}] - [\text{reference PEL average}]}{[\text{reference PEL average}]} \quad (2)$$

Linear approximations for the normalized reflection contrast were done as follows:

$NRC = -0.00089\theta - 0.00218$ for the 500-550 nm bandpass filter, and

$NRC = 0.00138\theta + 0.00175$ for the 570-600 nm bandpass filter.

Although calculated reflection spectra of plasmonic crystals provide insight into the complicated optical behaviors under different wavelength ranges, these computational results are not enough to describe the contrast changes on reflection images. The simulation assumes that the incident light is normal to the surface. Experimentally, the illumination angle of light radiated through an objective lens with a numerical aperture of 0.40 should be more than zero (maximum angle of 24°), which significantly influences the optical behavior of plasmonic crystals. We also did not consider effects due to light refraction at the air/ASW interface, using instead a modeled light source located in the ASW phase. This assumption reduces the complexity and computation time, but causes some deviation from the experimentally obtained results.

Cell Culture of *Aplysia californica* Pedal Ganglion Neurons. *Aplysia californica* sea slugs (100-300g) were supplied by the National Resource for *Aplysia* (Miami, FL) and kept in circulated, aerated seawater at 14 °C. Prior to dissection, the animals were anesthetized by

injection of isotonic magnesium chloride solution into the body cavity (~30-50 % of body weight). Individual *Aplysia* pedal neurons were isolated after a 60-120 min treatment at 34 °C of the ganglia with 1% solution of protease type XIV (Sigma-Aldrich) dissolved in ASW (in mM; 460 NaCl, 10 KCl, 10 CaCl₂, 22 MgCl₂, 26 MgSO₄, and 10 HEPES, pH 7.8) as described previously.^{7,8} A poly-L-lysine layer (1-2 nm) was formed on the plasmonic crystal surface. The cells were mechanically isolated from the protease treated ganglia in ASW, transferred onto the plasmonic crystal surface immersed in ASW supplemented with antibiotics (ASW containing 100 units/ml penicillin G, 100 µg/ml streptomycin, and 100 µg/ml gentamicin, pH 7.7) and left to attach and grow overnight at room temperature. Six to eight pedal neurons were cultured on the plasmonic crystal surface at a time. Measurements were only made within experiments for cells cultured on plasmonic crystals in which no damage-specific morphological changes, such as blebbing and neurite varicosation, were in evidence.

Atomic Force Microscopy of Fixed Neuron Cells on Plasmonic Crystals. Due to the limitations on live cell imaging using AFM, cultured *Aplysia* neurons on plasmonic crystals were fixed and dried before AFM measurements. Cells were fixed by addition of 1 mL of 4% paraformaldehyde to 3 mL antibiotic-supplemented ASW and occasional stirring for 30 s, removal of 1mL of the solution, addition of another 1mL of the 4 % paraformaldehyde solution and exposure for 30 s, followed by the removal of all solution. The cells were then carefully rinsed with deionized water and dried. Height profiles of fixed *Aplysia* neurons on the surface of the plasmonic crystal were measured using an Asylum Research MFP-3D atomic force microscope operated in tapping mode. Analysis of the AFM data was performed using IgorPro.

Cell Dissociation from Plasmonic Crystal Surface via Trypsinization. Cell detachment was induced by addition of trypsin into the ASW culture media. Trypsin was dissolved in ASW to reach a concentration of 10 mg/mL. For the detachment of *Aplysia* neuronal cells from the substrate, 0.3 mL of the trypsin solution were added into 3mL of antibiotic-supplemented ASW in which the plasmonic crystal with cultured live cells was immersed. Three to four cells were selected for analysis at a time. The evolution of the temporal response of the trypsin exposure is one expected for *Aplysia* neurons. These cells are significantly different from mammalian cells, by reasons of cell rigidity and extracellular matrix physicochemical properties. Most importantly, the measurement was performed at room temperature, where lower activity is expected in comparison with experiments with mammalian cell cultures that are typically carried out at 37°C.⁹

Finite-Difference Time-Domain (FDTD) Simulations of Plasmonic Nanostructures. Multiple 3D FDTD simulations were carried out to model the zero-order reflection/transmission spectra (with light normally incident on the glass substrate) and to verify optical behavior changes as a function of thin film thickness on a plasmonic crystal using a commercial FDTD software package, Lumerical FDTD (Lumerical Solutions Inc., Vancouver, Canada). The unit cell geometry defined a gold nanohole in the x-y plane with a 740 nm center-to-center hole spacing, a 545 nm hole diameter, a 280 nm relief depth, a 44 nm Au film on the top surface of the plasmonic crystal, a 16 nm Au film conformally coating the nanohole sidewalls, and a 16 nm Au film on the bottom of the nanoholes. The frequency dependent dielectric constant of gold was modeled using previously reported parameters from a Drude plus two-pole Lorentzian model.^{10,1} The refractive indices of NOA, polyelectrolyte, refractive index-corrected material for live cell, and ASW were set to be 1.56, 1.48, 1.42, and 1.34, respectively.

References:

1. Le, A. P.; Kang, S.; Thompson, L. B.; Rubakhin, S. S.; Sweedler, J. V.; Rogers, J. A.; Nuzzo, R. G. Quantitative Reflection Imaging of Fixed *Aplysia californica* Pedal Ganglion Neurons on Nanostructured Plasmonic Crystals. *J. Phys.Chem. B* 2013, *117*, 13069-13081.
2. Stewart, M. E.; Mack, N. H.; Malyarchuk, V.; Soares, J. A. N. T.; Lee, T. W.; Gray, S. K.; Nuzzo, R. G.; Rogers, J. A. Quantitative multispectral biosensing and 1D imaging using quasi-3D plasmonic crystals. *P. Natl. Acad. Sci. USA* **2006**, *103*, 17143-17148.
3. Yao, J. M.; Stewart, M. E.; Maria, J.; Lee, T. W.; Gray, S. K.; Rogers, J. A.; Nuzzo, R. G. Seeing molecules by eye: Surface plasmon resonance imaging at visible wavelengths with high spatial resolution and submonolayer sensitivity. *Angew. Chem. Int. Edit.* **2008**, *47*, 5013-5017.
4. Stewart, M. E.; Anderton, C. R.; Thompson, L. B.; Maria, J.; Gray, S. K.; Rogers, J. A.; Nuzzo, R. G. Nanostructured plasmonic sensors. *Chem. Rev.* **2008**, *108*, 494-521.
5. Stewart, M. E.; Yao, J. M.; Maria, J.; Gray, S. K.; Rogers, J. A.; Nuzzo, R. G. Multispectral Thin Film Biosensing and Quantitative Imaging Using 3D Plasmonic Crystals. *Anal. Chem.* **2009**, *81*, 5980-5989.
6. Yao, J. M.; Le, A. P.; Gray, S. K.; Moore, J. S.; Rogers, J. A.; Nuzzo, R. G. Functional Nanostructured Plasmonic Materials. *Adv. Mater.* **2010**, *22*, 1102-1110.
7. Ye, X. Y.; Xie, F.; Romanova, E. V.; Rubakhin, S. S.; Sweedler, J. V. Production of Nitric Oxide within the *Aplysia californica* Nervous System. *ACS Chem. Neurosci.* **2010**, *1*, 182-193.
8. Wang, L. P.; Ota, N.; Romanova, E. V.; Sweedler, J. V. A Novel Pyridoxal 5'-Phosphate-dependent Amino Acid Racemase in the *Aplysia californica* Central Nervous System. *J. Biol. Chem.* **2011**, *286*, 13765-13774.
9. Sizer, I. W. and Josephson, E. S. Kinetics as a function of temperature of lipase, trypsin, and invertase activity from —70 to 50°C.(—94 to 122°F.). *J. Food Sci.* **1942**, *7*: 201–209
10. Aldred, N.; Ekblad, T.; Andersson, O.; Liedberg, B.; Clare, A. S. Real-time quantification of microscale bioadhesion events in situ using imaging surface plasmon resonance (iSPR). *ACS Appl. Mater. Interfaces* **2011**, *3* (6), 2085–2091.

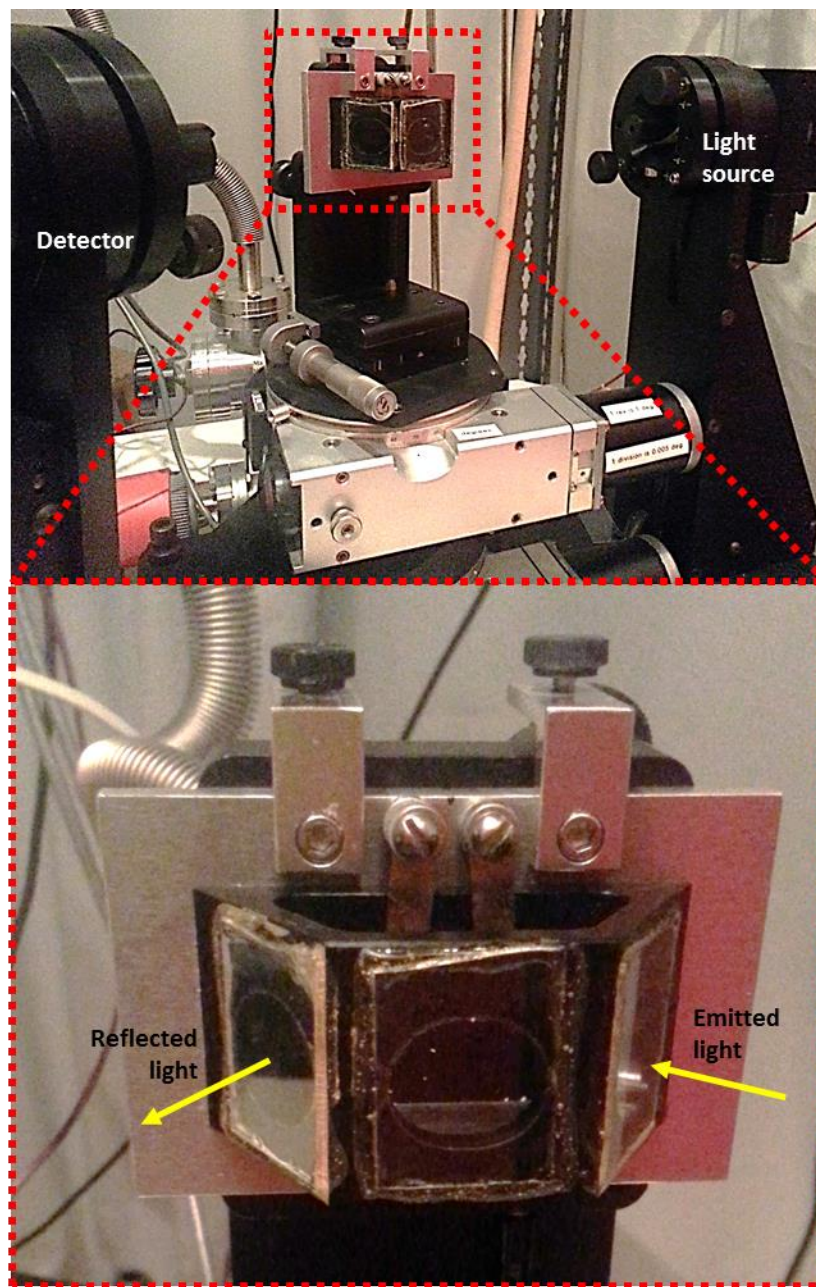


Figure S1. Digital picture of a home-built liquid cell for ellipsometry.

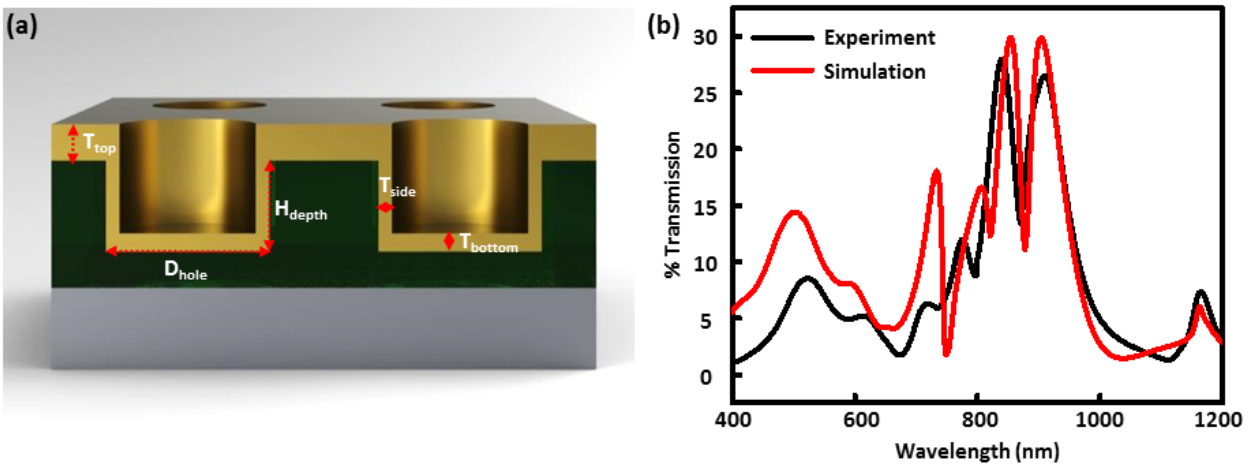


Figure S2. (a) Schematic illustration of the cross section of the 3D plasmonic crystal used for FDTD modeling. The full 3D plasmonic crystal with the periodicity of hole of 740 nm, hole depth (H_{depth}) of 280 nm, and diameter of hole (D_{hole}) of 545 nm are used for all FDTD calculations. For simplicity, we assumed that the metal films are uniformly distributed on NOA nanoholes with a right angle edge; the thickness of the Au layer on top surface of the crystal (T_{top}) and on the sidewall (T_{side}) and bottom (T_{bottom}) of the nanoholes are 44, 16, and 16 nm, respectively. (b) Experimental transmission spectra (black) and FDTD calculated transmission spectra (red) of full 3D plasmonic crystal.

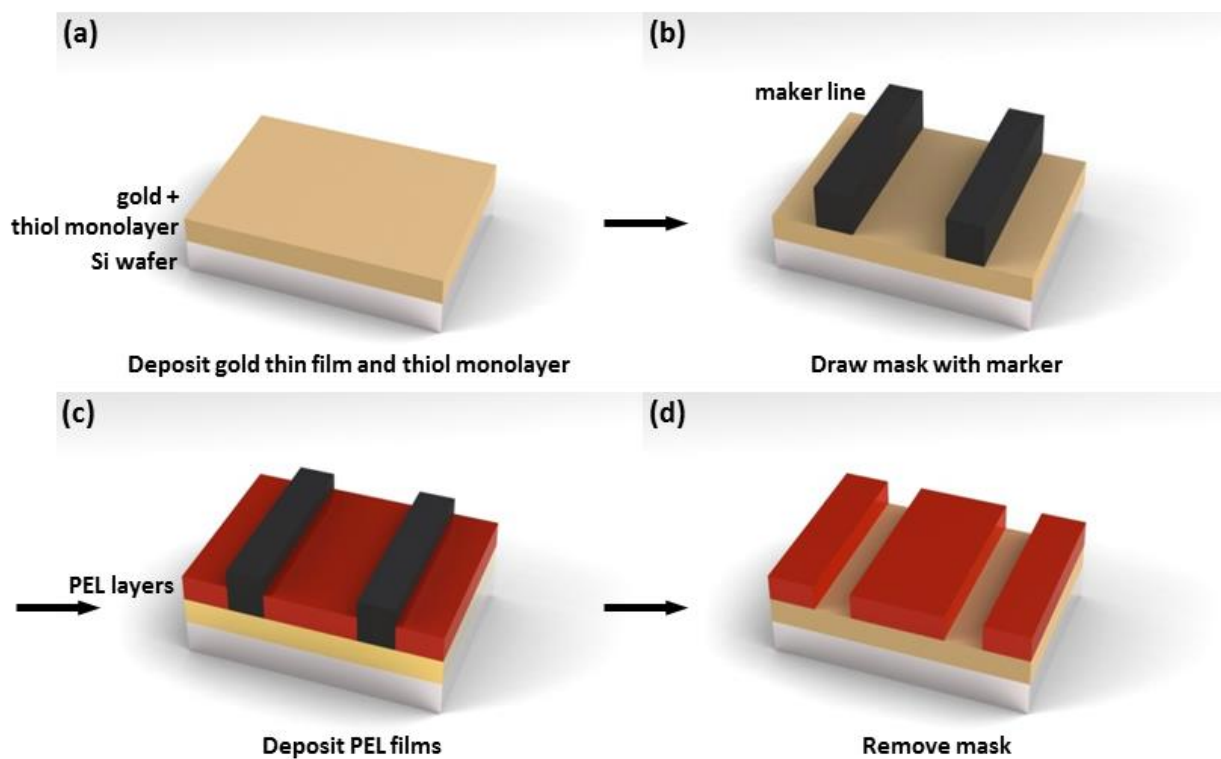


Figure S3. Schemes of the polyelectrolyte film patterning process using a permanent marker: (a) MHDA monolayer is formed on gold-coated silicon wafer by immersing the substrate in ethanolic solution of MHDA (2 mM). (b) Lines are drawn with a permanent marker on a substrate to be used as a mask for polyelectrolyte deposition. (c) Polyelectrolyte assemblies are grown on the substrate through the layer-by-layer method. (d) Permanent marker mask is removed by rinsing with acetone.

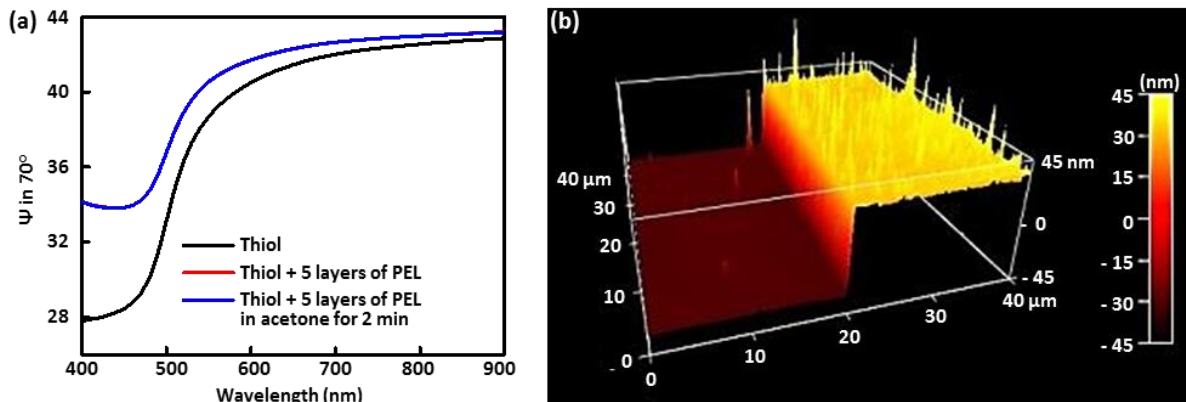


Figure S4. (a) Three ellipsometric spectra of gold-coated silicon piece with MHDA monolayer; measured before polyelectrolyte deposition, after 5 layers of PAH/PSS deposition, and following immersion in acetone. Ellipsometric spectra of gold-coated silicon piece immersed in acetone for 2 min (red trace) is obscured by ellipsometric data obtained after 5 layers of PAH/PSS deposition (blue trace). (b) 3D AFM image of the step edge of a polyelectrolyte pattern made by the deposition of 18 layers of PAH/PSS.

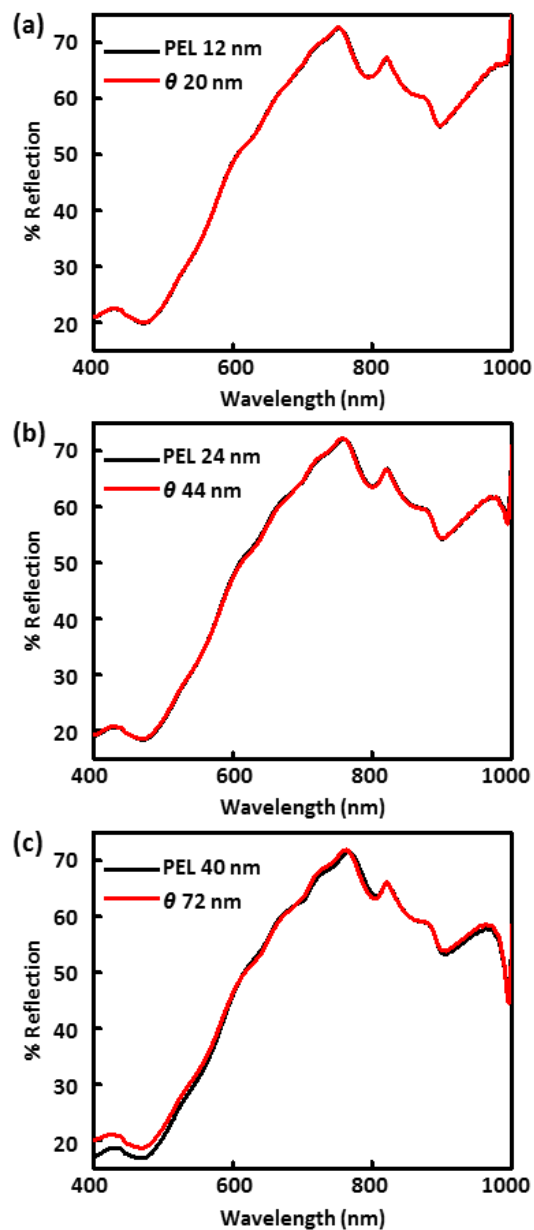


Figure S5. FDTD simulated reflection spectra for pairs of optically equivalent polyelectrolyte (black trace) and index-corrected material for the live cell conformally covering a full 3D plasmonic crystal (red trace): (a) 12 nm polyelectrolyte and 20 nm index-corrected material; (b) 24 nm polyelectrolyte and 44 nm index-corrected material; (c) 40 nm polyelectrolyte and 72 nm index-corrected material.

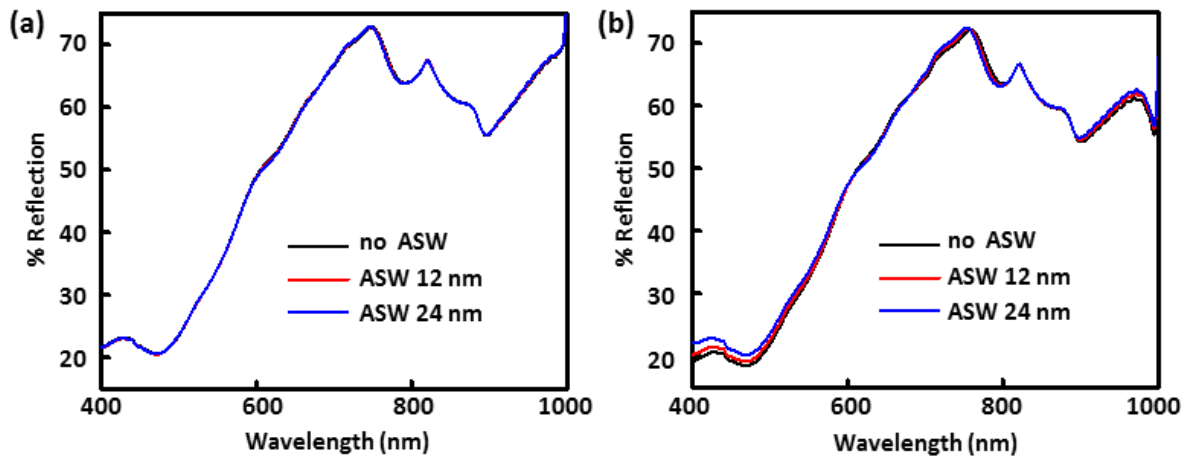


Figure S6. FDTD simulated reflection spectra for different thickness of ASW gap (0, 12, and 24 nm of ASW gap) between plasmonic crystal and (a) 20 nm of index-corrected material or (b) 40 nm of index-corrected material.

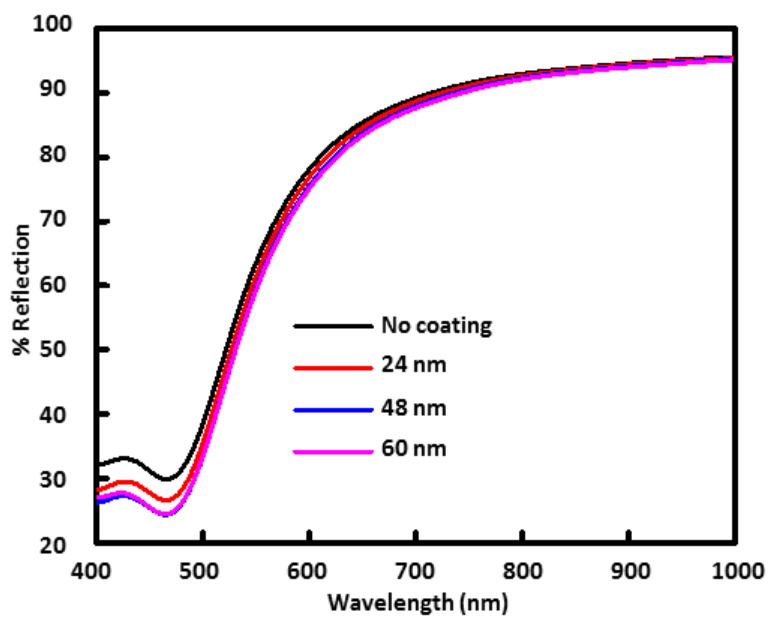


Figure S7. FDTD calculated reflection spectra for varying thicknesses of index-corrected material on flat gold film.

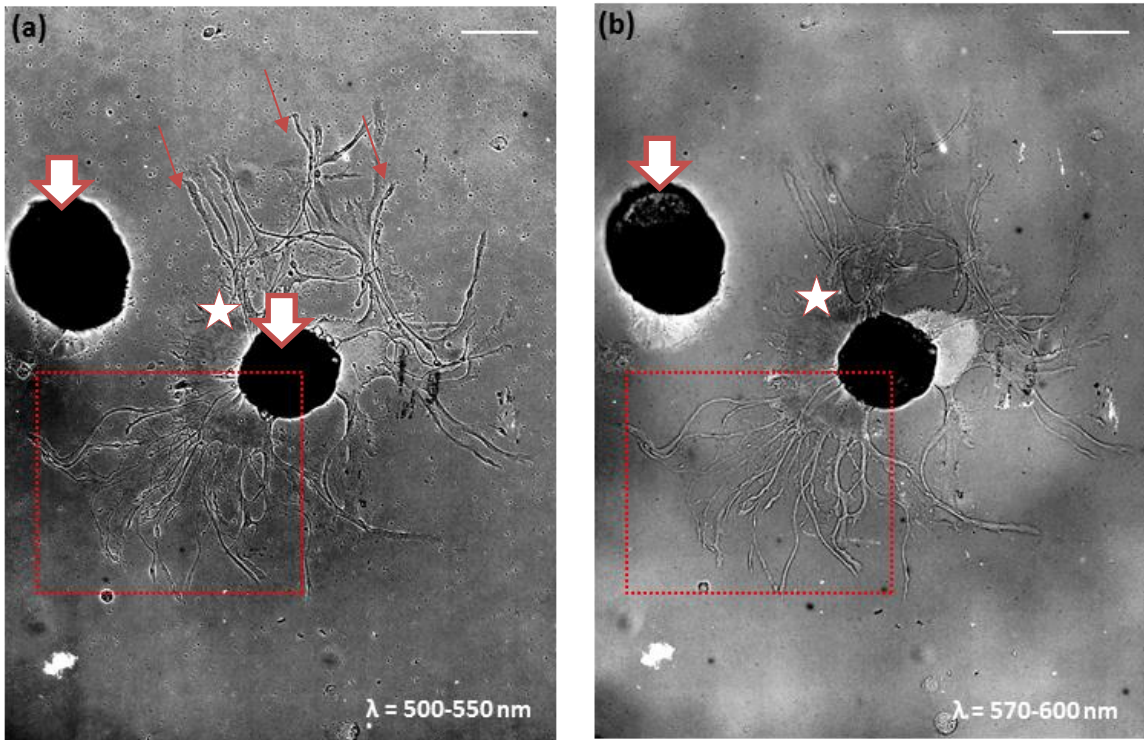


Figure S8. Raw reflection image of live *Aplysia* neuronal cells cultured on a plasmonic crystal acquired using (a) a 500-550 nm bandpass filter and (b) a 570-600 nm bandpass filter. The scale bar corresponds to 100 μm . The regions in the red boxes are magnified and presented in Figure 2. Thick arrows mark cell bodies. Thin arrows indicate examples of neuronal processes. Star is placed on representative examined thin region near the cell body

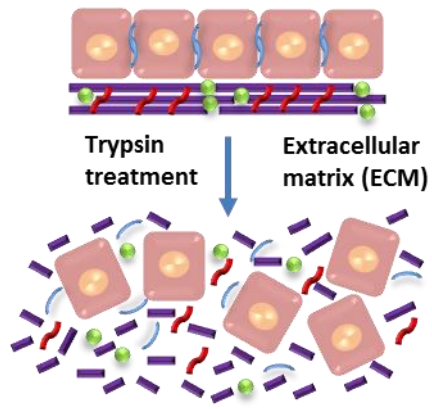


Figure S9. Schematic of cell detachment induced by trypsinization.

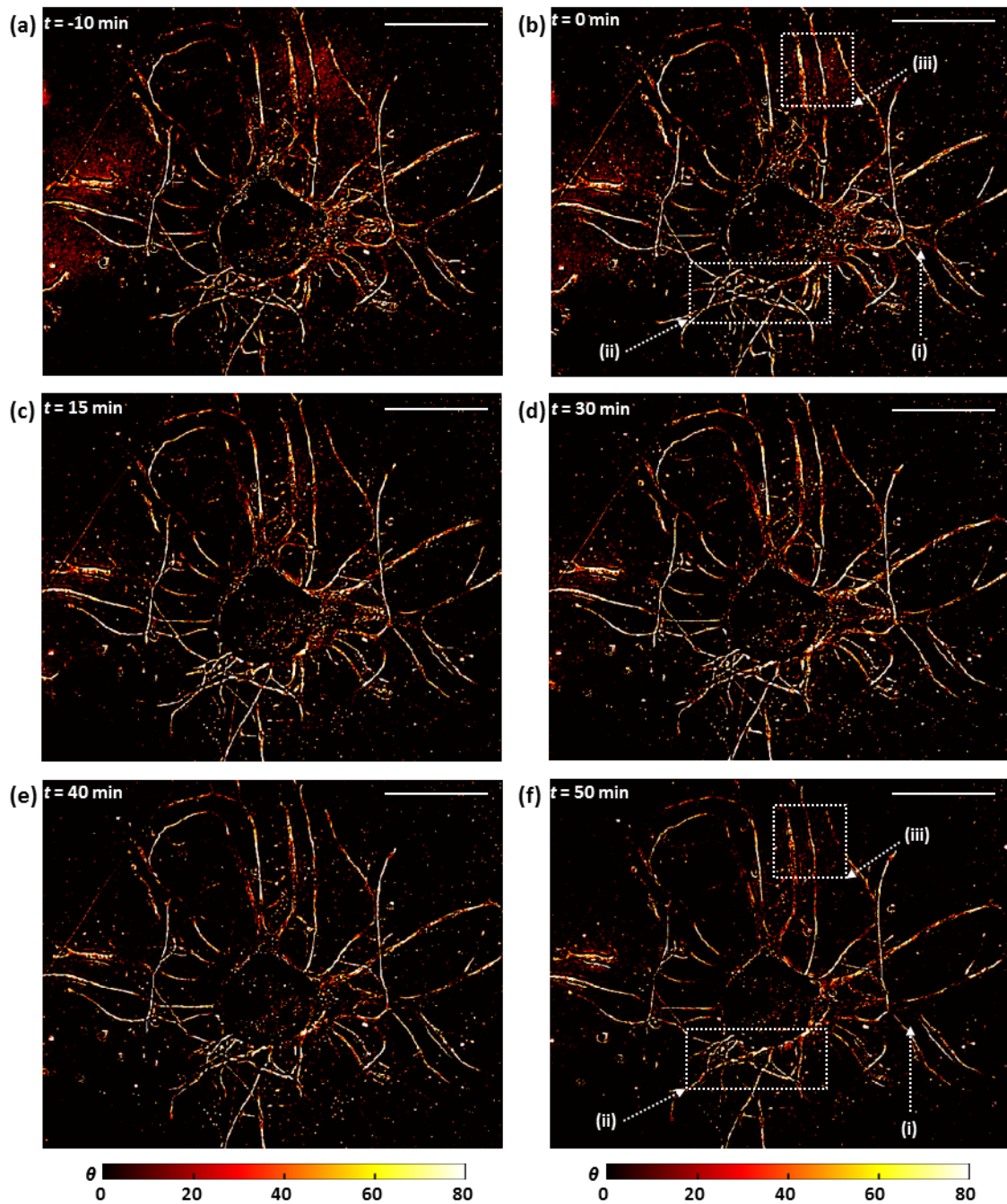


Figure S10. Mass coverage transformed images of the live *Aplysia* neuron acquired for time-lapse analysis of cell detachment induced by trypsinization. Dotted-line boxes mark regions with neuronal processes characterized by distinguishable changes in contrast profiles over time. The scale bars correspond to $100 \mu\text{m}$.

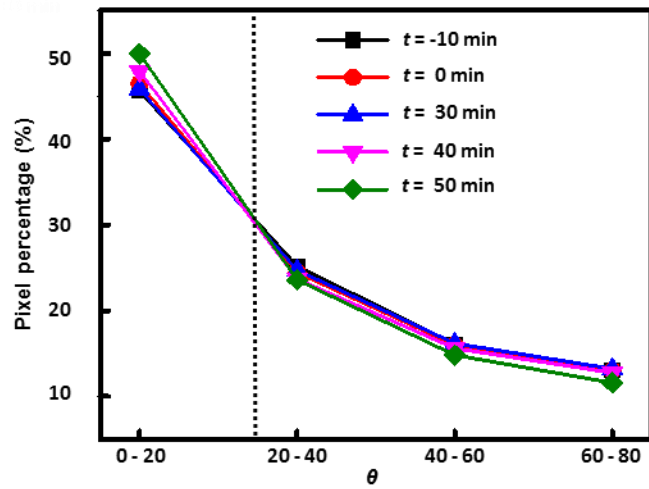


Figure S11. Pixel percentage distributions across various ranges of θ values of mass coverage transformed images of the live *Aplysia* neuron acquired for time-lapse analysis of cell detachment induced by trypsinization. The dotted line represents the θ value corresponding to the inversion point of the observed trend.

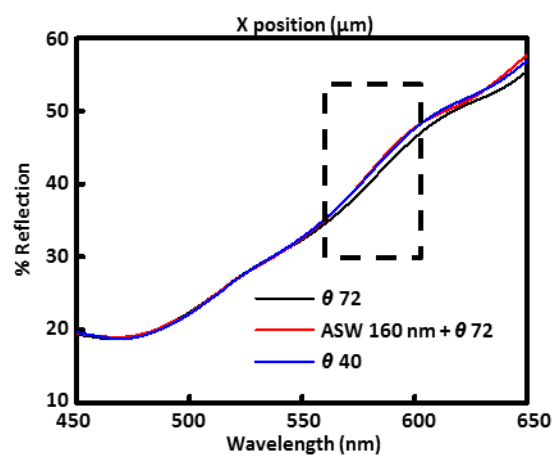


Figure S12. Three reflection spectra of plasmonic crystals covered with 72 of index corrected mass coverage, 160 nm ASW gap between plasmonic crystal and 72 of index corrected mass coverage, and 40 of index corrected mass coverage. The dotted-line square shows that the 570-600 nm range is best for observing the difference in reflection values induced by the ASW layer inserted between the cell and the plasmonic crystal.